JMEPEG (2008) 17:849–856
DOI: 10.1007/s11665-008-9244-2

1059-9495/$19.00

Research on Transient Liquid Phase Diffusion Bonding of Steel Sandwich Panels Under Small Plastic Deformation

H. Li and Z. X. Li

(Submitted September 3, 2007; in revised form March 20, 2008)

Plastic deformation was newly introduced in transient liquid phase (TLP) diffusion bonding of steel sandwich panels. The effect of plastic deformation on bonding strength was investigated through lab experiments. It was assumed that three factors, including newly generated metal surface area, deformation heat, and lattice distortion, contribute to the acceleration of interface atoms diffusion and increase of diffusion coefficients. A numerical model of isothermal solidification time was developed for TLP bonding process under plastic deformation and applied to carbon steel sandwich panels bonding with copper interlayer. A reasonable isothermal solidification time was obtained when an effective diffusion coefficient was used. Based on lab experiments, the effects of plastic deformation on interlayer film thickness and isothermal solidification time were studied through theoretical calculation with the new model. The evolution of interlayer film thickness indicates a good agreement between the calculation and experimental measurement. The results show that the isothermal solidification time is obviously reduced due to the effect of plastic deformation. Furthermore, a new steel sandwich cooling panel for heat exchanger was fabricated by TLP diffusion bonding under 13.1% plastic deformation. The test results suggest that a steel sandwich panel of inequidistant fin structure can provide enhanced heat transfer efficiency.

Keywords heat transfer performance, isothermal solidification, modeling, plastic deformation, sandwich panel, transient liquid phase diffusion bonding

1. Introduction

Transient liquid phase (TLP) diffusion bonding is a joining process that involves the formation of a metallurgical bond as the liquid interlayer solidifies isothermally with the diffusion proceeding when held at the bonding temperature (Ref 1-3). In conventional TLP bonding, it is considered that the liquid interlayer might ensure intimate contact at the joint interface at low bonding pressures. However, for TLP diffusion bonding of sandwich panels, the joining process must produce joints with adequate strength without significantly degrading the properties of the component materials (Ref 4). Thus, proper bonding pressure is favorable for improving the soundness of the joints.

For a given bonding temperature, an important process parameter in TLP diffusion bonding for sandwich panels is the holding time required to complete the isothermal solidification process (Ref 5). If isothermal solidification is not completed, the residual liquid in the interlayer solidifies as deleterious brittle eutectic phases during cooling, which causes deterioration of the mechanical properties of a joint (Ref 6). The experimental approach used to determine the holding time might be time consuming and costly. Simulation of isothermal solidification during TLP diffusion bonding is useful to determine the optimum holding time. A number of models based on migrating solid/liquid interface have been used by several researchers to analyse isothermal solidification process (Ref 5-11). It is assumed that the time for completion of isothermal solidification process is basically dependent on the solute diffusivity in the solid substrate and the phase relationships between interlayer material and base metal. However, the predicted time is usually long enough to discourage the potential applications of TLP in many industries (Ref 12). Therefore, to reduce the holding time, a better understanding of the effect of bonding pressure on the time required to complete isothermal solidification is necessary. By a combination of direct experimentation with computational modeling, the optimum holding time can be set prior to actual field trials.

Hence, in the present work, TLP diffusion bonding under certain plastic deformation, which indicates the influence of bonding pressure, was conducted to evaluate the suitability of the bonding process for the fabrication of steel sandwich panels, and the effect of plastic deformation on the joint strength was investigated. A mathematical model was established to calculate the time required to complete isothermal solidification, and the predicted results were compared with experimental investigations. Additionally, a steel sandwich panel for cooling was fabricated by TLP diffusion bonding under certain plastic deformation and its heat transfer performance was analyzed.

H. Li and **Z. X. Li**, Research Institute of Advanced Materials Processing Technology, Beijing University of Technology, Pingleyuan 100, Chaoyang District, Beijing 100022, China. Contact e-mail: hongli@bjut.edu.cn.

2. Experimental and Investigations

2.1 Experimental Procedures

Honeycomb core sandwich panels were 100 mm by 100 mm and consisted of two 2 mm-thick steel face sheets TLP bonded to a 5 mm-thick honeycomb core. The materials used for face sheet and honeycomb core were commercial cold rolled carbon steel DQ (Drawing Quality) sheet. The chemical compositions and mechanical property are given in Table 1. A pure Cu foil of 50 μm thickness was selected as interlayer material. The surfaces to be bonded were ground and then degreased using acetone. To apply plastic deformation on honeycomb core panel, a vacuum furnace equipped with a roller was designed to carry out TLP bonding. Samples were heated to bonding temperature and then isothermally held for a certain time. To observe the bonding interface during a TLP bonding process, the samples should be quenched at the end of the isothermal holding stage. However, quenching of samples was quite difficult because of the furnace mechanics. Therefore, in this work, to apply plastic deformation and quenching, TLP diffusion bonding was performed in Gleeble 1500 thermal simulator, as illustrated in Fig. 1. The heating rate (3.5 °C s^{-1}) was kept constant for all the processes, and the vacuum level was approximately maintained at 1×10^{-5} torr.

The specimen was heated to the bonding temperature 1100 °C and immediately compressed under given reduction 0%, 5%, 8%, 15%, 18%, and 25%, respectively, then held for 30 min at 1100 °C while the load began to decrease, and finally water quenched.

The interface bonding strength was estimated by measuring the average shear strength of the joints on MTS 810 material test machine. For each test, three samples under the same processing condition were taken. Microstructural observations were performed using an optical microscope (OM), and interlayer film thicknesses of the joints were measured by scanning electron microscope (SEM).

Table 1 Chemical compositions and mechanical property of DQ carbon steel

Chemical compositions, wt.%							Tensile strength σ_b, MPa	Yield strength σ_s, MPa
C	Si	Mn	P	S	AlN	Ca		
0.051	0.032	0.181	0.009	0.006	0.031	0.0024	325	210

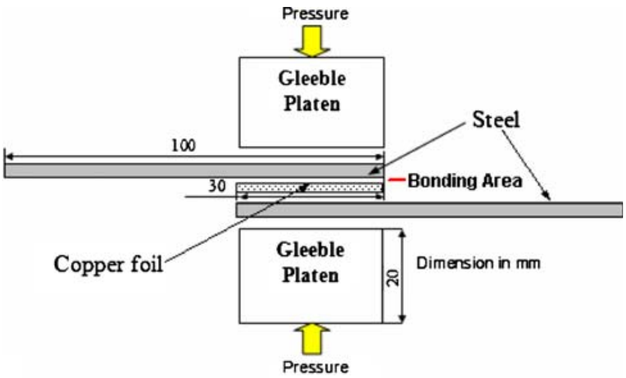

Fig. 1 Geometrical configuration in bonding and dimensions of specimen

2.2 Bonding Strength and Microcharacteristics of the Joints

Samples were taken out after TLP bonding test, and the actual reductions were measured according to the thickness changes of samples. The measured reductions were 0%, 4.5%, 5.8%, 13.1%, 14.0%, and 22%, respectively. Figure 2 shows the interface bonding strength at different measured reductions. It can be seen that when plastic deformation increases from 0% to 13.1%, the bonding strength increases with the reduction and reached the maximum of 228.6 MPa at reduction 13.1%. The bonding strength under nil reduction was 143.2 MPa, which was only 68.2% of that of the base metal. However, the joint has the maximum strength exceeding that of the base metal by nearly 8.8%. It suggests that firm metallurgical bond forms in the interface. When the reduction increases, it leads to a decrease of the film thickness.

As indicated before, for steel sandwich panel, too large plastic deformation may destruct the original configuration and performance of honeycomb core, but too little plastic deformation could not get the allowable bonding strength. In the present experiment, neither failure in the profile nor degradation in properties of honeycomb core was observed. Thus, 13.1% is the most appropriate reduction for achieving high strength and maintaining good configuration of honeycomb core.

Figure 3 shows an OM micrograph of a cross section of the TLP-bonded joint under different plastic deformation. Figure 4 shows SEM images of the bonding interface under reduction 5.8% and 13.1%. It can be seen that the bond-line almost disappeared and the bonding area was homogeneous in grain structure under reduction 13.1% as compared to that without reduction.

The actual film thickness of the interlayer film after isothermal diffusion with a 30-min holding time under different reduction was measured using SEM, as shown in Fig. 5. It can be seen that when plastic deformation increased from 0% to 13.1%, the measured film thickness decreases with reductions. It reaches the minimum 4.8 μm at 13.1% reduction. The decrease of film thickness corresponds to the increase of bonding strength. When reduction increases to a high value, such as 22%, it leads to a remarkable increase of film thickness.

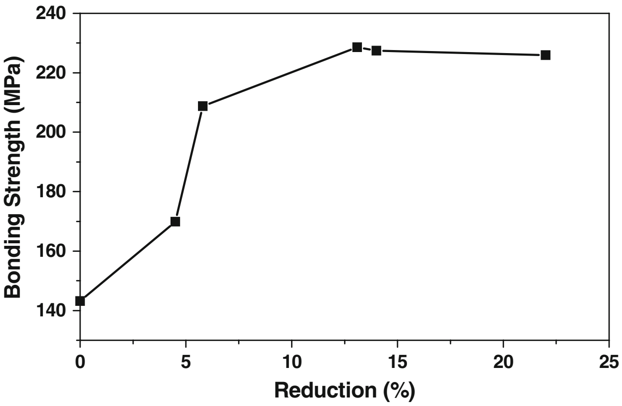

Fig. 2 The effect of plastic deformation on bonding strength

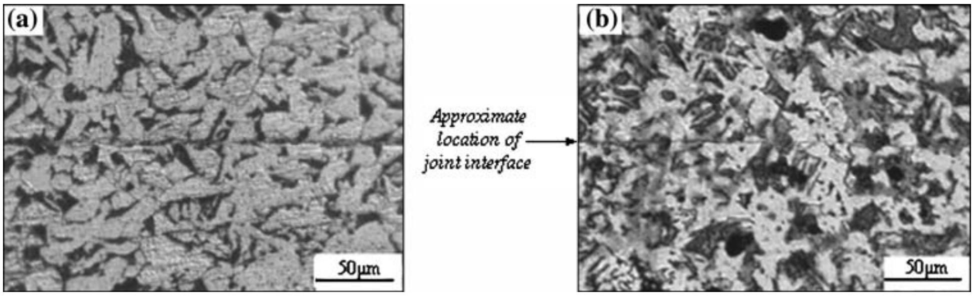

Fig. 3 Optical micrographs of bonded interface under (a) reduction 0% and (b) measured reduction 13.1%

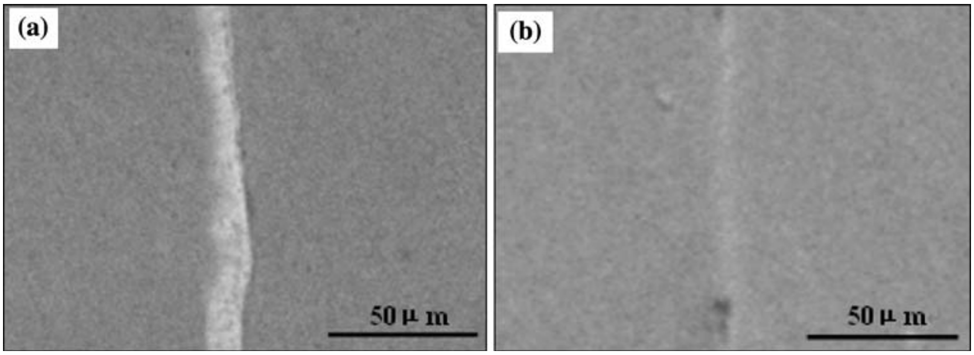

Fig. 4 SEM micrographs of bond interface under (a) reduction 0% and (b) measured reduction 13.1%

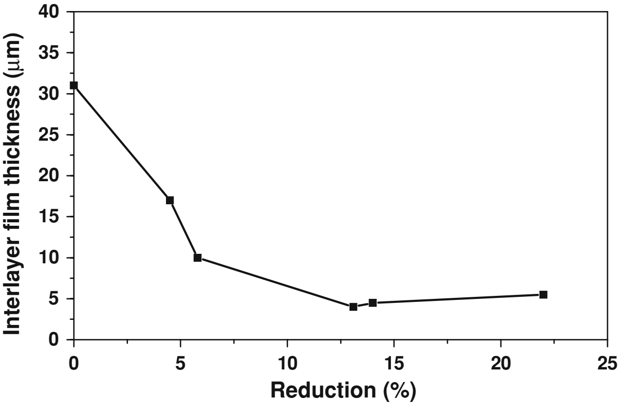

Fig. 5 The effect of plastic deformation on measured interlayer film thickness

2.3 Mechanism Analysis

Based on lab experimental investigations, it can be confirmed that plastic deformation accelerates the interlayer elements diffusion in base metal, resulting in increase of bonding strength and decrease of the film thickness. The effect of plastic deformation was explained as follows. First, the plastic deformation makes fresh metal and the flattened asperities are surrounded with the bands of newly generated surface area. The expanded surface to be joined becomes smoother than the initial undeformed one; thus it is beneficial for the activation and acceleration of atom interdiffusion across interface. Second, the plastic deformation causes deformation heat; it accumulates on the interface and leads to higher diffusion bonding temperature in interface area. Finally, plastic deformation causes lattice distortion and the atoms deviate from their equilibrium positions, which results in reduction of activation energy. The above three factors all contribute to the acceleration of interlayer atoms diffusion into base metal and increase of diffusion coefficients. Therefore, when plastic deformation was between nil and 13.1%, the TLP diffusion bonding process is speeded up. During holding stage, the liquid interlayer homogenizes and quickly isothermally solidifies and thus metallurgical bond is finally formed across interface area.

Additionally, it can be found that the interlayer film was almost in mirror symmetry with bonding strength. The interlayer film thickness begins to increase and the bonding strength begins to decrease when the reduction exceeds 13.1%. Under certain plastic deformation, the grain boundary density increases in each unit volume of solid phase. Because the diffusivity in grain boundary area is higher than that in the lattice area (intragranular area), the diffusion rate of Cu atoms in solid phase is increased. However, the excessively increased plastic deformation under high temperature might result in partial recrystallization of the base steel. Thus the grain size might increase during the process, resulting in an evident decrease in grain boundary density. Thus the Cu diffusion into steel might be delayed and the interlayer film thickness begins to increase.

3. Modeling of Isothermal Solidification Time

3.1 Model Establishment

The diffusion-controlled isothermal solidification stage of TLP diffusion bonding consists of a process that involves a moving solid-liquid interphase boundary. As was stated earlier, several models have been developed and proposed for estimating the time (t_{IS}) required to complete isothermal solidification based on the solution of Fick's second law (Ref 10). And the complete time for isothermal solidification t_{IS} is given by (Ref 4, 8, 9)

$$t_{IS} = \frac{\lambda_{1\max}^2}{16K^2D} \qquad \text{(Eq 1)}$$

where $\lambda_{l\max}$ is the maximum thickness of the liquid interlayer region at the end of widening and homogenization, D is the diffusion coefficient of the liquid interlayer in solid substrate, K is the constant which can be derived from Lesoult's demonstration (Ref 4, 13).

In the case of TLP diffusion bonding under plastic deformation, based on Tuah-Poku's estimation (Ref 4), the maximum thickness of the liquid interlayer $\lambda_{l\max}$ is given by the following equation applying mass balance method

$$\lambda_{1\max} = \lambda_0 \cdot (1-r) \cdot \left[1 + \left(\frac{\rho_b}{\rho_a}\right)\left(\frac{C_0 - C_{L\alpha}}{C_{L\alpha}}\right)\right] \qquad \text{(Eq 2)}$$

where λ_0 is the initial interlayer thickness, r is the measured reduction, ρ_b and ρ_a are density of the interlayer and base metal, respectively, $C_{L\alpha}$ is the solute concentration at which liquid interlayer begins to homogenize, and C_0 the initial solute concentration.

As the specimen is heated homogeneously in Gleeble, there are no temperature gradients existing in isothermal solidification process. However, in the case of TLP diffusion bonding under plastic deformation, as discussed previously, the actual bonding temperature in the faying interface might increase due to the deformation heat (Ref 14), and the temperature increment ΔT can be expressed by the equation

$$\Delta T = \frac{(1-f)}{c\rho}\bar{\sigma}(\varepsilon_1 - \varepsilon_0) \qquad \text{(Eq 3)}$$

where f is the fraction of the work stored, c is the specific heat per unit mass, ρ the density, $\bar{\sigma}$ the average stress, which can be calculated based on Hollomon strain-hardening equation (Ref 15), ε_0 the initial strain, and ε_1 the true strain.

Thus the diffusion coefficient of interlayer element in base metal at elevated bonding temperature can be described by the following equation

$$D = D_0 \exp\left(-\frac{Q}{R(T_b + \Delta T)}\right) \qquad \text{(Eq 4)}$$

where D_0 is pre-exponential factor and Q the activation energy, R is the gas constant, and T_b is the bonding temperature across interface area, which is measured directly by temperature transducer in Gleeble.

Therefore, the isothermal solidification time t_{IS} for TLP diffusion bonding under plastic deformation can be calculated according to the above equations. As mentioned before, t_{IS} is the most important factor determining the bonding time, thus if the holding time t_H in the experiment approaches or exceeds the calculated isothermal solidification time t_{IS} (i.e. $t_H \geq t_{IS}$), it means that the holding time is enough for the completion of isothermal solidification. If not, to gain solid metallic bonds, the holding time should be prolonged to complete the isothermal solidification process.

3.2 Application of Isothermal Solidification Time Model to Steel/Cu/Steel System

To apply the model developed above and compare it with experimental results for the steel/Cu/steel system, the following assumptions were included:

- During the rapid heating up stage, Cu diffusion was considered negligible. During isothermal solidification process, the solid-liquid interface was considered of local equilibrium, the temperature and concentration distributions in the liquid regions were flat, and no constitutional undercooling occurred in the liquid.
- Since Fe is the base element in carbon steel, the Fe-Cu binary phase diagram was used to establish the concentration values $C_{L\alpha}$ and C_0 at the bonding temperature: $C_{L\alpha}$ = 96.7%, and C_0 = 100% (Ref 10, 16). The values for the densities of Cu and DQ carbon steel are given as $\rho_{Cu} = \rho_b = 8.96$ kg m^{-3} and $\rho_{steel} = \rho_a = 7.86$ kg m^{-3}.
- As the base metal is a polycrystalline structure, which is composed of only α-ferrite and a little perlite in room temperature, diffusion coefficient of Cu measured in pure α-Fe is applicable. When the bonding temperature increases to 1100 °C, the ferrite in DQ carbon steel transforms into austenite. Based on Majima's measured results, pre-exponential factor $D_0 = 4.16 \times 10^{-4}$ m^2 s^{-1} and activation energy Q = 305 kJ mol^{-1} for the lattice diffusion of Cu in γ-Fe (Ref 17).

Consequently, according to Eq 2, when reduction is 13.1%, the maximum thickness of the liquid phase $\lambda_{l\max}$ was calculated as $\lambda_{l\max}$ = 45.23 μm.

In the present study, to effectively control the deformation and stabilize diffusion bonding process, low strain rate (0.001 s^{-1}) was applied to complete the required strain, and the maximum load was 26844.7 N. The load-time diagram and stress-strain curve under hot deformation are shown in Figs. 6 and 7, respectively. From the obtained strain-hardening curve of base metal under bonding temperature T_b = 1100 °C, the average flow stress $\bar{\sigma}$ under different true stain ε can be calculated. In this case, the bonding temperature is so high that the fraction of the work stored f is equal to zero. The specific heat per unit mass of base metal is 0.45 J g^{-1} K^{-1}. Thus, according to Eq 3, the temperature increment ΔT caused by deformation heat under reduction 13.1% was calculated as follows: ΔT = 2.8 K.

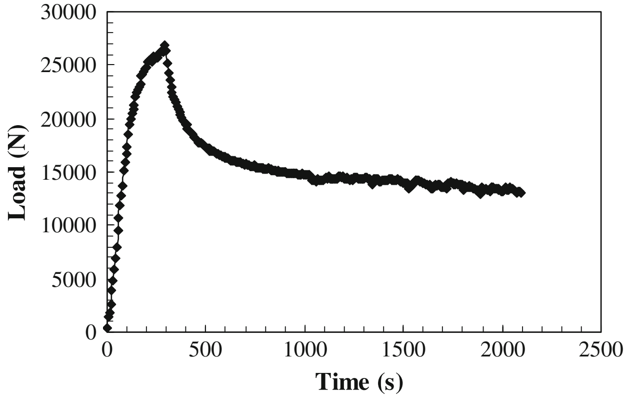

Fig. 6 Load-time curve

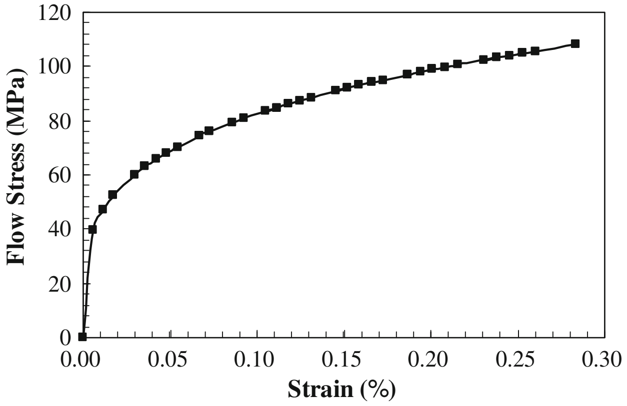

Fig. 7 Stress-strain curve under hot deformation

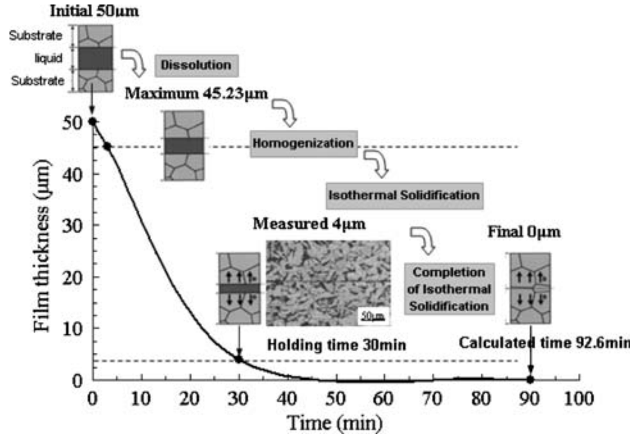

Fig. 8 Evolution of profile of interlayer film thickness

Table 2 Summary of time estimations for isothermal solidification

Case Number	Diffusion mechanism	Diffusion coefficient of Cu used, m^2/s	t_{IS} model	Time ratio $R = t_{IS}/t_H$
1	Lattice diffusion	$D^{Cu}_{lattice-Fe}$: 1.08×10^{-15}	7.9×10^5 min (548.0 days)	2.63×10^4
2	Grain boundary diffusion	D^{Cu}_{gb-Fe}: 1.84×10^{-10}	4.6 min	0.15
3	Contribution of both lattice and grain boundary diffusion	D^{Cu}_{mean}: 4.45×10^{-13} (a) D^{Cu}_{eff}: 9.18×10^{-12} (b)	1.9×10^3 min (1.3 days) 92.6 min	64.1 3.10

(a) Geometric mean $D^{Cu}_{mean} = \sqrt{D^{Cu}_{lattice-Fe} \cdot D^{Cu}_{gb-Fe}}$

(b) Effective diffusion coefficient of Cu according to equation (Ref 16): $D_{eff} = D_{lattice} + D_{gb} \cdot (2\delta/d)$, where δ is the effective grain boundary thickness and d the average grain diameter. In this case $\delta/d = 0.025$ according to the experimental measurements

However, as Zhou et al. had indicated, when a polycrystalline metal is TLP diffusion bonded, diffusion coefficient of the solute is much higher in grain boundary than in the bulk material when the bonding temperature is in the range 0.5-$0.75T_m$ (where T_m is the melting temperature in K) (Ref 18). Since the bonding temperature T_b (1373 K) is approximately $0.77T_m$ of DQ carbon steel (close to the upper end where grain boundary diffusion is the dominant factor), three different diffusion mechanisms—only lattice diffusion, only grain boundary diffusion, and contribution of both—were considered in the calculation of diffusion coefficient for t_{IS} estimation.

Based on the above analysis, isothermal solidification time estimations obtained from the application of established model are summarized in Table 2, considering the different Cu diffusion coefficient under reduction 13.1%. Time ratio R is the ratio of predicted time t_{IS} to the experimental holding time t_H.

It could be seen that big differences in time estimations for isothermal solidification are obtained when diffusion coefficients are changed (from minutes, as in case 2 and 3-b, to several days, as in case 1 and 3-a). It varied significantly from experimental results (i.e. $t_H = 30$ min). This might be explained due to the differences between diffusion coefficients for lattice and grain boundary diffusion mechanism. For a polycrystalline metal, the grain boundary, which represents the fastest path for diffusion of Cu atoms, is many times larger than the surface area, and diffusion coefficient is much higher along grain boundaries than in the lattice structures; thus, solid-state diffusion takes place through both the lattice and grain boundaries to achieve isothermal solidification (Ref 18). This is further proved with the calculation results when different diffusion coefficients for combined diffusion mechanism are used in the model (i.e. case 3-a and 3-b). In the former case, the geometric means diffusion coefficient D^{Cu}_{mean} considered both lattice diffusion and grain boundary diffusion in γ-Fe to have the same influence on the bonding process, and a time ratio of 64.1 was obtained, while in the latter case, the effective diffusion coefficient D^{Cu}_{eff} considered the contribution of both grain boundary thickness and grain size, and a time ratio of 3.1 was obtained. It shows a good approximation of the experimental results. In consequence, based on the above discussions, it suggests that the most appropriate diffusion coefficient of Cu in γ-Fe during isothermal solidification might be the effective diffusion coefficient.

3.3 Comparison of Isothermal Solidification Time Under Different Plastic Deformation

Based on the interlayer film thickness measured by SEM and estimation results of isothermal solidification time, the evolution of interlayer film thickness during TLP diffusion bonding process is illustrated in Fig. 8. The curve gives a quantitative representation of the effect of bonding time on interlayer film thickness.

At the beginning of plastic deformation, the initial thickness of the interlayer film was 50 μm. Thereafter, when the bonding temperature increased to 1100 °C, the interlayer began to melt. The dissolution of interlayer was so rapid that homogenization of the liquid phase was completed in a few minutes. At the same time, under certain plastic deformation (r = 13.1%), the liquid zone reached its maximum thickness 45.23 μm as calculated. After isothermal diffusion with a 30-min holding time, the measured thickness of the interlayer film decreased to 4 μm. Finally, the thickness of the film decreased to 0 μm at the predicted time 92.6 min, indicating the completion of isothermal solidification. From the profile, it can be seen that the theoretically calculated curve was in good agreement with the experimental measurements. Furthermore, the experimental holding time is less than the calculated isothermal solidification time (i.e. $t_H < t_{IS}$), and it indicates that after a bonding time 30 min, the joint region has not completely solidified, this confirms the expectation that prolonging the appropriate holding time by 60 min might help to complete the whole isothermal solidification.

Additionally, the effect of plastic deformation on interlayer film thickness and isothermal solidification time was studied. As shown in Fig. 9 (i.e. case a and c), based on the established model, under the same conditions of initial interlayer thickness (λ_0 = 50 μm), bonding temperature (T_b = 1373 K), and holding time (t_H = 30 min), the liquid zone homogenized to the maximum thickness λ_{lmax} = 52.05 μm (under reduction 0%) while λ_{lmax} = 45.23 μm (under reduction 13.1%). Correspondingly, isothermal solidification time t_{IS} predicted with the effective diffusion coefficient is as follows: t_{IS} = 129.6 min (under reduction 0%) while t_{IS} = 92.6 min (under reduction 13.1%). In addition, if the bonding temperature was only increased by the temperature increment ΔT (2.8 K) with nil plastic deformation (i.e. case b), the maximum interlayer thickness λ_{lmax} = 52.05 μm while t_{IS} = 123 min. A more likely explanation for the differences between the values obtained was given. Under plastic deformation, deformation heat is enhanced, which results in quick increase of temperature increment ΔT. Hence, the actual bonding temperature across interface is increased, and Cu diffusion into steel is accelerated. However, the temperature increment ΔT is not the dominant factor.

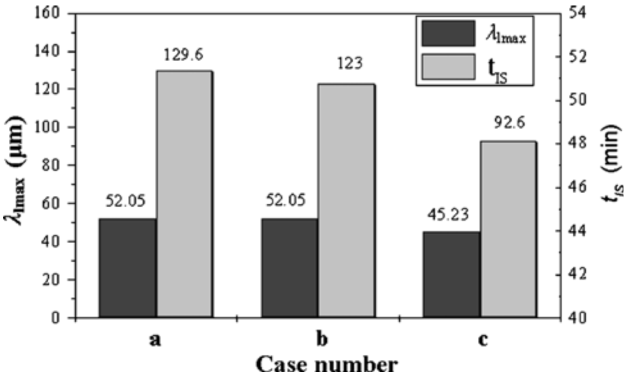

Fig. 9 The calculated maximum thickness of liquid interlayer and predicted isothermal solidification time under different plastic deformation (a) $r = 0\%$, $T = 1373$ K; (b) $r = 0\%$, $T = 1375.8$ K, and (c) $r = 13.1\%$, $T = 1375.8$ K

Under plastic deformation, the grain boundary density increases in each unit volume of solid phase. Because the diffusivity in grain boundary area is higher than that in the lattice area (intragranular area), the diffusion rate of Cu atoms in solid phase is increased. On the other hand, the plastic deformation under high temperature could result in partial recrystallization of the steel. In this case, the migration of grain boundary would accelerate the diffusion process. Thus Cu diffusion into steel is greatly enhanced and the time for isothermal solidification is evidently decreased in comparison with that in conventional TLP bonding condition without plastic deformation.

In the previous research work on TLP diffusion bonding, Tuah-Poku et al. had predicted isothermal solidification time in Ag/Cu/Ag system, where a ratio (i.e. estimated time/experimental time) of 6.0 was obtained (Ref 3). The big difference might be in part due to the nonplanar nature of the bond region. Nevertheless, only a few work considered the influence of lattice diffusion and grain boundary diffusion. Padron et al. had modeled the TLP behavior in DSS/Cu/DSS system (Ref 10). A good agreement between the time calculated for isothermal solidification and experimentally observed was obtained (the time ratio ranges from 1.0 to 1.1) when a geometric mean of diffusion coefficient was estimated. The results suggest that lattice and grain boundary diffusion plays a dominant role during the TLP bonding process. However, in the present study, the effect of plastic deformation on TLP diffusion bonding was considered in isothermal solidification time simulations. It is obvious that certain plastic deformation accelerates the interlayer diffusion into base metal, which results in evident shortening of the isothermal solidification process.

4. Application of TLP Bonding on Fabricating Steel Sandwich Panels

High efficiency use in heat exchangers demands components of lightweight and high performance in mechanical, automobile, and aerospace field. Heat transfer operations can be intensified through the use of compact heat exchangers. In particular, plate-fin heat exchangers offer many advantages over conventional designs (Ref 19).

Based on the lab experiment and model analyzing, a new steel sandwich cooling panel for heat exchanger was designed and fabricated. Face sheet (1 mm-thick) and core panel were all made of cold-rolled carbon steel DQ sheets. Two typical core panels with plain-fin structures were designed. The structural parameters are shown in Table 3. Plain-fin core panel (sample 1) has an equidistant fin structure while panel (sample 2) has a nonequidistant fin structure. The assembled face sheet and core

Table 3 Structural parameters of plain-fin core panel

Sample number	Core length *L*, mm	Core width *B*, mm	Fin height *H*, mm	Fin thickness *t*, mm	Fin spacing *W*, mm	Heat transfer area F_i, 10^4 mm^2	Ratio of secondary surface area to total surface area *i*
1	140	100	10	1.0	5	0.0052	0.692
2	140	100	10	0.5	2 (wide side); 5 (narrow side)	0.0090	0.833

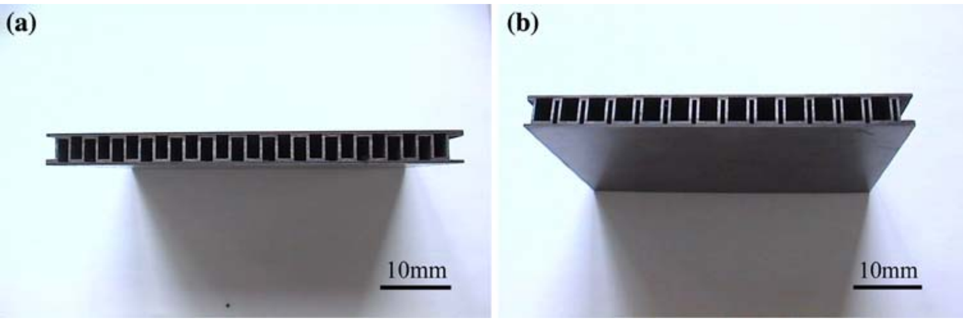

Fig. 10 Photographs of steel sandwich cooling panels (a) specimen 1 and (b) specimen 2

panel were TLP diffusion bonded by a 50 μm-thick Cu interlayer in a vacuum furnace equipped with a roller. The parameters are as follows: bonding temperature 1100 °C; reduction 13.1%; holding time 93 min. The photographs of fabricated steel sandwich cooling panels are shown in Fig. 10.

The shear test shows that a sound metallurgical bond has formed between face sheet and core panel with a bonding strength of 228.5 MPa, which is suitable for high temperature and high pressure flow.

To compare the efficiency of two different types of steel sandwich cooling panels, their heat transfer performances was tested and analyzed. Heat transfer coefficients of cooling panels were calculated according to equation (Ref 5):

$$h = \frac{Q}{F\Delta t_m} \qquad \text{(Eq 5)}$$

where F is the heat transfer surface area, Q is the heat capacity, and Δt_m the temperature difference between inlet and outlet fluid.

Tests on heat transfer coefficient were carried out in the following conditions: atmospheric pressure 763 mmHg; room temperature 29–30 °C and relative humidity (RH) 40-50%.

Figure 11 shows the heat transfer coefficients calculated in waterside and air side, respectively, when the heat capacity is 550 W and the recycled cooling water temperature is 55 °C. It can be seen that under the different flux, the heat transfer coefficients in both water side and air side are much higher in specimen 2 than that in specimen 1. It illustrates that the heat transfer performance of steel sandwich panels with nonequidistant fins is better than that with equidistant fins at constant temperature. The reason accounting for the result is that the heat transfer surface area and the ratio of secondary surface area to the total surface area in specimen 2 is larger than those in specimen 1 (see Table 3).

The test result also shows that when there is a pinpoint change in flux, change of heat transfer coefficient in airside is observable while change of heat transfer coefficient in waterside is not observable. The waterside is currently in laminar flow with lower velocity and thus the heat transfer effect is not evident. If the velocity is increased for the flow in waterside to reach turbulent flow, the heat transfer coefficient in waterside could be greatly increased. As the heat transfer coefficient in airside is much higher than that in waterside under constant temperature, enhancing heat transfer in airside might achieve a good result. It could also be presumed that steel sandwich cooling panel with nonequidistant fin structure is more suitable to be used in gas-gas exchange environment, for example, acting as aircraft engine parts.

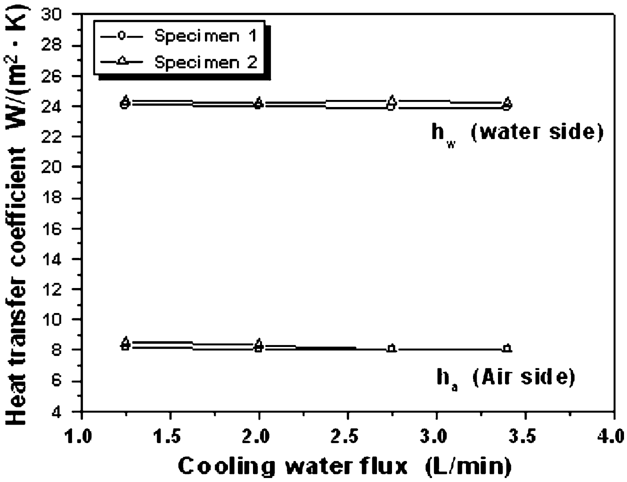

Fig. 11 Comparison of heat transfer coefficients at recycled water temperature 55 °C

5. Conclusions

Plastic deformation was newly introduced in TLP diffusion bonding of steel sandwich panels. It was observed that the joint had the maximum strength and the minimum interlayer film thickness when plastic deformation was 13.1%. It is supposed that three important factors, including newly generated metal surface area, deformation heat, and lattice distortion account for the acceleration of interface atoms diffusion and increase of diffusion coefficients.

The kinetics of isothermal solidification during TLP bonding of steel/Cu/steel system under plastic deformation was studied through migrating liquid/solid interface modeling and solute distribution law. When reduction increased from nil to 13.1%, the calculated values t_IS predicted with the effective diffusion coefficient decreased from 129.6 to 92.6 min. The result suggests that plastic deformation might significantly shorten the isothermal solidification process.

The evolution of interlayer film thickness during TLP diffusion bonding process indicates a good agreement between the time calculated for isothermal solidification and experimental results. However, the experimental holding time is less than the calculated isothermal solidification time; it suggests that after a bonding time 30 min, the joint region has not completely solidified, and thus the appropriate holding time should be prolonged to finish the whole isothermal solidification.

Furthermore, a reasonable isothermal solidification time was obtained when the effective diffusion coefficient was used. The results suggest that under plastic deformation, lattice diffusion and grain boundary diffusion through the γ-Fe in carbon steel jointly play an important role in TLP diffusion bonding process at bonding temperature of 1100 °C.

Based on the lab experiment and model analyzing, a new steel sandwich cooling panel for heat exchanger was fabricated by TLP diffusion bonding under 13.1% plastic deformation. An improved steel sandwich panel of inequidistant fin structure was designed and provided enhanced heat transfer efficiency.

Acknowledgment

The authors acknowledge the support of National 863 Program and Beijing PHR (IHLB) Project.

References

1. W.F. Gale and D.A. Butts, Overview Transient Liquid Phase Bonding, *Sci. Technol. Weld. Joining*, 2004, **9**, p 283–300
2. J.D. Sugar, J.T. Mckeown, T. Akashi, S.M. Hong, K. Nakashima, and A.M. Glaeser, Transient-Liquid-Phase and Liquid-Film-Assisted Joining of Ceramics, *J. Euro. Cera. Soc.*, 2006, **26**, p 363–371
3. M.D. Tuah-Poku and T.B. Massaliski, A Study of the Transient Liquid Phase Bonding Process Applied to a Ag/Cu/Ag Sandwich Joint, *Metall. Trans. A*, 1988, **19**, p 675–686
4. R.K. Bird and E.K. Hoffman, *NASA Report L-17717*. NASA, Washington DC, 1998, p 26
5. N.L.R. Ojo and M.C. Chaturvedi, Effect of Gap Size and Process Parameters on Diffusion Brazing of Inconel 738, *Sci. Technol. Weld. Joining*, 2004, **9**, p 532–540
6. M.A. Arafin, M. Medraj, D.P. Turner, and P. Bocher, Transient Liquid Phase Bonding of Inconel 718 and Inconel 625 with BNi-2: Modeling and Experimental Investigations, *Mater. Sci. Eng. A*, 2007, **447**, p 125–133
7. Y. Natsume, K. Ohsasa, and T. Narita, Numerical Modeling of the Transient Liquid-Phase Diffusion Bonding Process of Al Using Cu Filler Metal, *ISIJ Int.*, 2003, **12**, p 1976–1982
8. Y. Zhou, W.F. Gale, and T.H. North, Modelling of Transient Liquid Phase Bonding, *Int. Mater. Rev.*, 1995, **40**, p 181–196
9. W.D. MacDonald and T.W. Eagar, Isothermal Solidification Kinetics of Diffusion Brazing, *Metall. Mater. Trans. A*, 1996, **29**, p 315–325
10. C.E. Campbell and W.J. Boettinger, Transient Liquid-Phase Bonding in the Ni-Al-B System, *Metall. Trans. A*, 2000, **31**, p 2835–2842
11. T. Padron, T.I. Khan, and M.J. Kabir, Modelling the Transient Liquid Phase Bonding Behaviour of a Duplex Stainless Steel Using Copper Interlayer, *Mater. Sci. Eng. A*, 2004, **385**, p 220–228
12. T.C. Illingworth, I.O. Golosnoy, and T.W. Clyne, Modelling of Transient Liquid Phase Bonding in Binary Systems—A New Parametric Study, *Mater. Sci. Eng. A*, 2007, **445–446**, p 493–500
13. G. Lesoult, *Center for Joining of Materials Report*. Carnegie Mellon University, Pittsburgh, 1996, p 14
14. G.J. Richardson, D.N. Hawkins, and C.M. Sellars, *Worked Examples in Metalworking*. The Institute of Metals, London, 1985, p 34
15. J.H. Hollomon and L.D. Hollomon, Time-Temperature Relations in Tempering Steel, *Trans. AIME*, 1945, **162**, p 223–249
16. T.B. Massalski, T.L. Murray, H.L. Bennett, and H. Baker, *Binary Alloy Phase Diagrams*. American Society for Metals, Metals Park, OH, 1986, p 56
17. K. Majima, S. Orito, and H. Mitani, Lattice and Grain Boundary Diffusion of Cu in γ-Fe, *Trans. Jpn. Inst. Met.*, 1978, **9**, p 663–668
18. Y. Zhou, Analytical Modeling of Isothermal Solidification During Transient Liquid Phase (TLP) bonding, *J. Mater. Sci. Lett.*, 2001, **20**, p 841–844
19. K.A. Thole and Daniel D.G. Knost, Heat Transfer and Film-Cooling for the Endwall of a First Stage Turbine Vane, *Int. J. Heat Mass Transfer*, 2005, **48**, p 5255–5269